Supporting Information

Girard et al. 10.1073/pnas.1719029115

SI Materials and Methods

***nbs-1(me102)* Isolation, Mapping, and Identification.** *nbs-1(me102)* was isolated in a genetic screen for meiotic mutants exhibiting altered numbers and/or appearance of GFP::COSA-1 foci. The AV727 strain used for this screen allowed simultaneous live imaging of GFP::COSA-1 foci, chromatin (mCherry::H2B), and germ cell membranes (GFP::PH). F1 progeny of ethyl methanesulfonate (EMS) mutagenized parents were plated individually, and pools of adult F2 progeny from each F1 plate were mounted on multiwell slides in anesthetic (0.1% tricaine and 0.01% tetramisole in M9 buffer) to visualize their germ lines; candidate mutations were recovered from siblings of visualized worms. *me102* was balanced by the *mIn1 (II)* balancer and then mapped to an ∼6.8-cM region on chromosome II between *unc-4* and *rol-1*. After backcrossing (three times) to generate the AV828 strain, homozygous *me102* worms were subjected to whole-genome sequencing. DNA was extracted from ∼400 individually picked *me102* homozygous or AV727 gravid adult worms, which were rinsed twice in M9 and resuspended in 10 mM EDTA and 0.1 M NaCl. Worms were then pelleted; flash frozen in liquid nitrogen; resuspended in 450 μL of lysis buffer containing 0.1 M Tris, pH 8.5, 0.1 M NaCl, 50 mM EDTA, and 1% SDS plus 40 μL of 10 mg/mL proteinase K in TE (10 mM Tris, 1 mM EDTA), pH 7.4; vortexed; and incubated at 62 °C for 45 min. Two successive phenol-chloroform extractions were performed using the Phase Lock gel tubes from Invitrogen, and DNA was precipitated with 1 mL of 100% ethanol plus 40 μL of saturated NH_4Ac (5 M) and 1 μL of 20 mg/mL GlycoBlue. The DNA pellet was washed with 70% ethanol, air dried, and resuspended in 50 μL of TE, pH 7.4. Paired end libraries were prepared using the Nextera technology (Illumina), and sequencing was performed on an MiSeq sequencer (2 × 75 bp). Reads were mapped to *C. elegans* reference genome (WBcel 235) using Bowtie software. Variant calling was performed using UnifiedGenotyper software from GATK (https://software.broadinstitute.org/gatk), and lists from AV828 and AV727 were compared to eliminate non-causal SNPs and insertion and/or deletion mutations (INDELs). Two mutations in the 6.8-Mb interval on chromosome II were specific to the *me102* strain. Both were canonical EMS-induced G > A or C > T mutations: one a missense mutation in the *C07E3.3* gene and the other a nonsense mutation in the *C09H10.10* gene.

CRISPR Genome Editing. We used direct injection of Cas9 protein (PNAbio) complexed with single-guide RNA (sgRNA) generated by in vitro transcription from a PCR template. CRISPR targeting (crRNA) sequences were designed using either Benchling (https://benchling.com/) or ChopChop (chopchop.cbu.uib.no/) following guidelines from ref. 1. crRNA sequences used to generate *me103*, *me104*, *me105*, and *me106* alleles were GAGCATAGAATGGGGCGATG and GTTCATGCGAGCATAGAATG (Fig. S1). dsDNA template for RNA transcription was obtained by PCR amplification using a "universal" reverse primer (oCG83: AATTTCACAAAAAGCACCGACTCGGTGCCACTTTTT CAAGTTGATAACGGACTAGCCTTATTTTAACTTGCTATTTCTAGCTCTAAAAC) and a forward primer containing the T7 promoter sequence upstream of the crRNA sequence as well as 20 bp of complementarity with oCG83 (namely oCG84 TAATACGACTCACTATAGGGGAGCATAGAATGGGGCGATGGTTTTAGAGCTAGAAAT; and oCG85: TAATACGACTCACTATAGGGGTTCATGCGAGCATAGAATGGTTTTAGAGCTAGAAAT). PCR was performed with the Phusion master mix from NEB in 50 μL with 4 μL of each oligo (10 mM stock) using the following program: 94 °C for 5 min; 25 cycles of 94 °C for 30 s, 55 °C for 30 s, and 72 °C for 30 s; and ending by a step at 72 °C for 5 min. dsDNA was purified on column, and concentration was assessed by Nanodrop. In vitro transcription was done overnight using the Ambion MEGAscript Kit from ThermoFisher. Ensuing RNA purification was performed using the MEGAclear Kit with a final elution volume of 40 μL. Cas9/sgRNA complexes were formed for 10 min at room temperature with 500 ng/μL Cas9 protein (PNABio) and 250 ng/μL both sgRNA (total final concentration for both guides combined). N2 worms (P0) were injected with the mix along with pCJF104 as a coinjection marker (2). Red F1s (carrying pCJF204) were singled out, and a subset of F2 progeny was fixed and stained with DAPI (see *Materials and Methods*) to assess the phenotype of diakinesis nuclei. From plates containing worms exhibiting aggregated chromosomes at diakinesis, the new mutations were recovered from siblings of the imaged worms and balanced by *mIn1*. The *nbs-1* locus was amplified from homozygous mutant worms using oCG48 (GAGAAAGGCTCCGTGGTCAA) and oCG50 (GCCGTCAACTTCCAGAGTCA) primers and subjected to Sanger sequencing (Sequetech). Details of the mutations can be found in Fig. S1.

Yeast Two-Hybrid Experiments. Worm RNAs were extracted by adding 250 μL Trisol to 20 μL WT N2 worm pellet in M9 and incubating at 4 °C for 30 min followed by standard phenol-chloroform extraction (see above). cDNAs were obtained from these RNAs using the SuperScript III first-strand synthesis for RT-PCR by Invitrogen. cDNA sequences of MRE-11, RAD-50, COM-1, and NBS-1 were amplified using the following primers containing SpeI and AvrII restriction sites to allow for cloning into pDP133 (prey vector, complementing leucine auxotrophy) and pDP134-135 (bait vector, complementing tryptophan auxotrophy) (3).

MRE-11 forward: NNNNACTAGTATGTGTGGCAGTGA

MRE-11 reverse: NNNNCCTAGGTTAGAAGAAACTTAG

RAD-50 forward: CTAACTAGTATGGCGAAATTTTTACGCCTACAC

RAD-50 reverse: CTACCTAGGGAACCGTCTCTTCGTATTAACTCT

COM-1 forward: NNNNACTAGTATGCAATCTGTGGATCCATTTG

COM-1 reverse: NNNNCCTAGGTTAATTCCACGTATTGATTCCAGTCGG

NBS-1 forward: NNNNACTAGTATGCCCATCAATGGCATAAAAATCAAAAACTC

NBS-1 reverse: NNNNCCTAGGTCAGTGCACAATTCT

The plasmid bearing the mutated version of MRE-11 (MRE-11 *iow1*) was generated using Gibson assembly (NEB) to replace a 366-bp SpeI XbaI fragment from pDP133-MRE-11 with a corresponding dsDNA fragment containing the *iow1* mutation.

Yeast strain YCK580 was transformed according to ref. 4 with plasmid pairs, with one plasmid containing the prey fused with the GAL4 activation and the other containing the bait fused with the LexA DNA binding domain. Transformed cells were spread on selective media lacking both leucine and tryptophan (−LW) and grown for 48 h at 30 °C. One clone was selected for each pair, and interaction was assayed on media lacking histidine (−LWH) with or without the His3p competitive inhibitor 3-AT (25 mM).

1. Paix A, Folkmann A, Rasoloson D, Seydoux G (2015) High efficiency, homology-directed genome editing in *Caenorhabditis elegans* using CRISPR-Cas9 ribonucleoprotein complexes. *Genetics* 201:47–54.
2. Frøkjaer-Jensen C, et al. (2008) Single-copy insertion of transgenes in Caenorhabditis elegans. *Nat Genet* 40:1375–1383.
3. Kraft C, et al. (2012) Binding of the Atg1/ULK1 kinase to the ubiquitin-like protein Atg8 regulates autophagy. *EMBO J* 31:3691–3703.
4. Gietz RD, Schiestl RH (2007) High-efficiency yeast transformation using the LiAc/SS carrier DNA/PEG method. *Nat Protoc* 2:31–34.

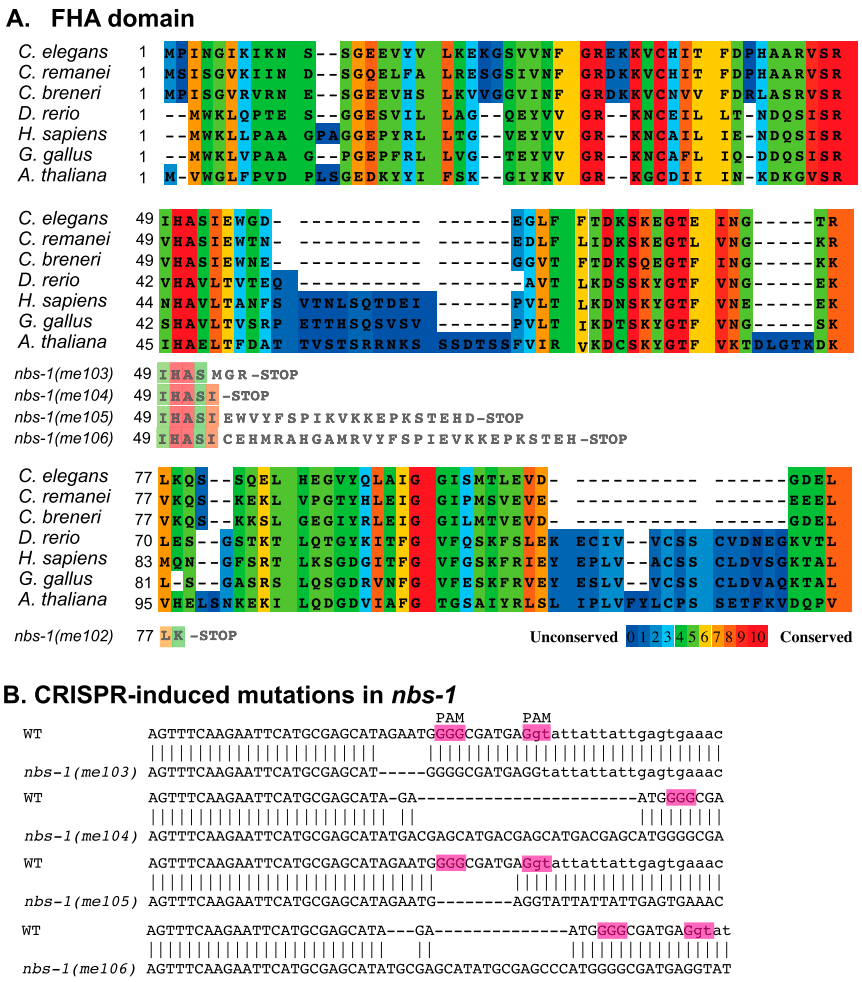

Fig. S1. Conservation among the NBS1/Nibrin protein family. (*A*) T-Coffee alignment showing conservation of the FHA domain among members of the NBS1/Nibrin protein family, with color coding generated using the PRALINE software. Predicted effects of *nbs-1* mutations obtained through EMS mutagenesis (*me102*) or CRISPR mutagenesis (*me103-me106*) on the protein sequence are also shown. Accession numbers are *Homo sapiens*, BAA28616.1; *Gallus gallus*, NP_989668.1; *Danio rerio*, NP_001014819.1; *Saccharomyces cerevisiae*, AAA35220.1; *Schizosaccharomyces pombe*, BAC80248.1; and *Caenorhabditis elegans*, NP_496374.2. (*B*) Genomic DNA sequence alignments between the WT *nbs-1* gene (starting at 179 bp after ATG) and *nbs-1* mutant alleles generated by CRISPR. The protospacer-adjacent motif (PAM) sequences (NGG) targeted are indicated in pink.

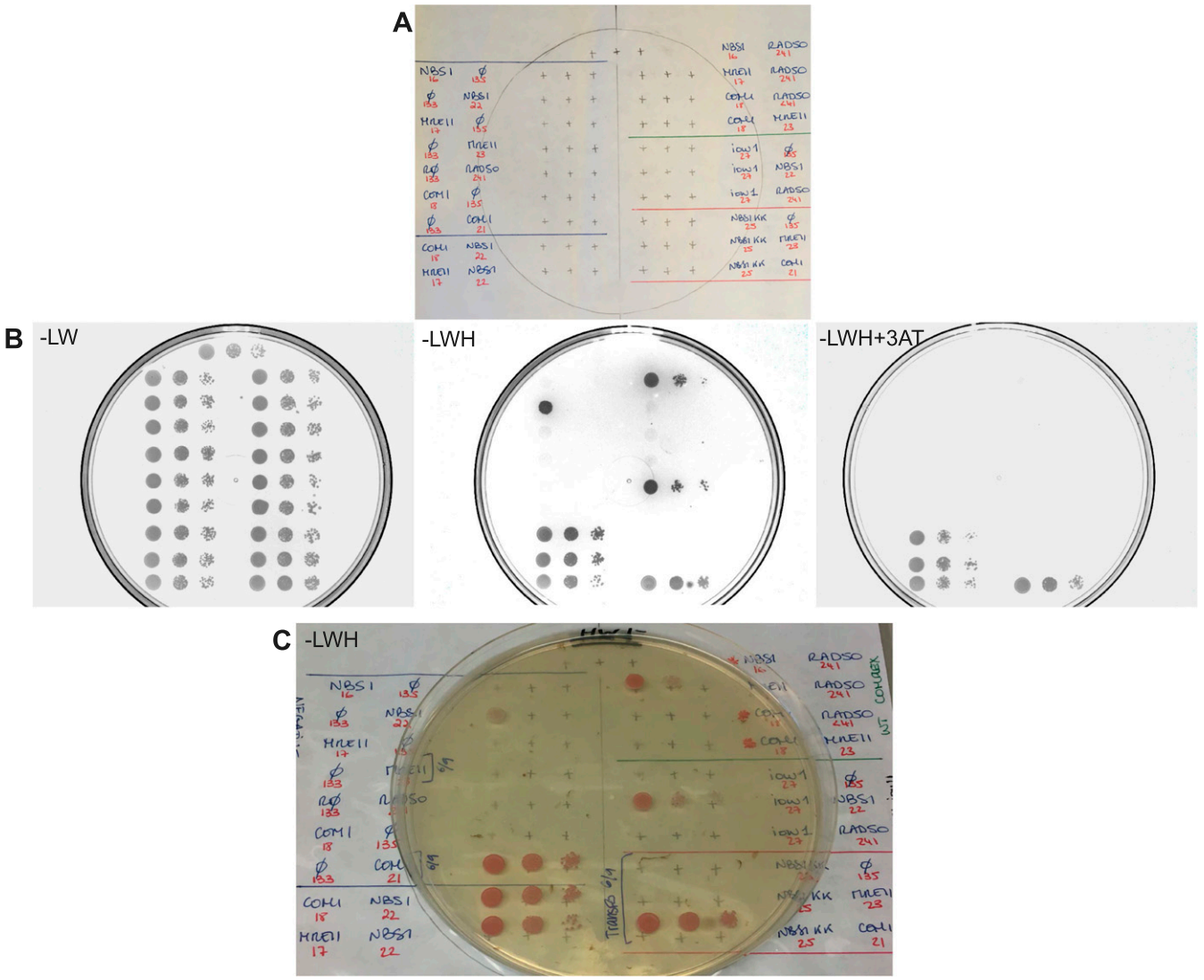

Fig. S2. Raw images for the yeast two-hybrid experiment presented in Fig. 1*E*. (*A*) Map showing all of the combinations plated in this experiment, with ∅ indicating empty vector (pDP133 if in *Left* or pDP135 if in *Right*); NBS-1 KK refers to a mutant version of NBS-1 (K236E K331E) affecting the MID (1). (*B*) Images captured using the BioRad Gel Doc XR+ system of all three plates spotted according to the map in *A* on SD-LW (growth test), SD-LWH (interaction test), or SD-LWH + 3-AT (interaction test). (*C*) Color picture of the SD-LWH plate superimposed on the map displayed in *A* for orientation. Genotypes that were uninformative either because of autoactivation from individual clones or because of failure to detect an interaction between WT NBS-1 in pDP133 and MRE-11 in pDP135 in separately plated positive controls were not included in Fig. 1*E*.

1. Kim JH, et al. (2017) The Mre11-Nbs1 interface is essential for viability and tumor suppression. *Cell Rep* 18:496–507.

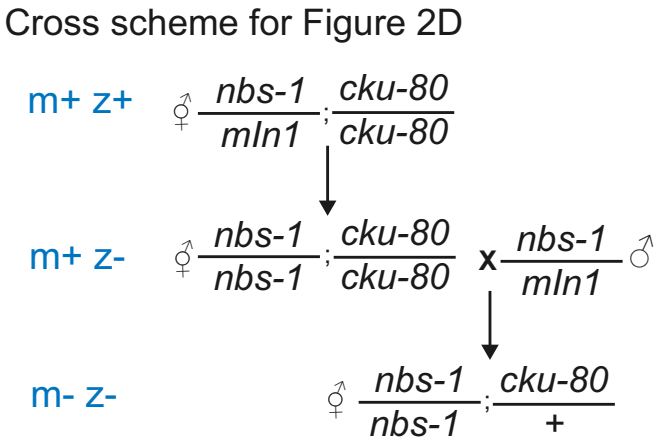

Fig. S3. Crossing strategy used for Fig. 2*D* to obtain homozygous *nbs-1(me102)* mutant worms from homozygous *nbs-1(me102)* mothers (m−z−). *mln1* refers to the balancer chromosome used to maintain the *nbs-1* mutation in a heterozygous state. Because progeny viability is partially restored in the *nbs-1; cku-80* double mutant (Table S1), viable m−z− *nbs-1* homozygotes that contained a WT *cku-80(+)* allele could be generated.

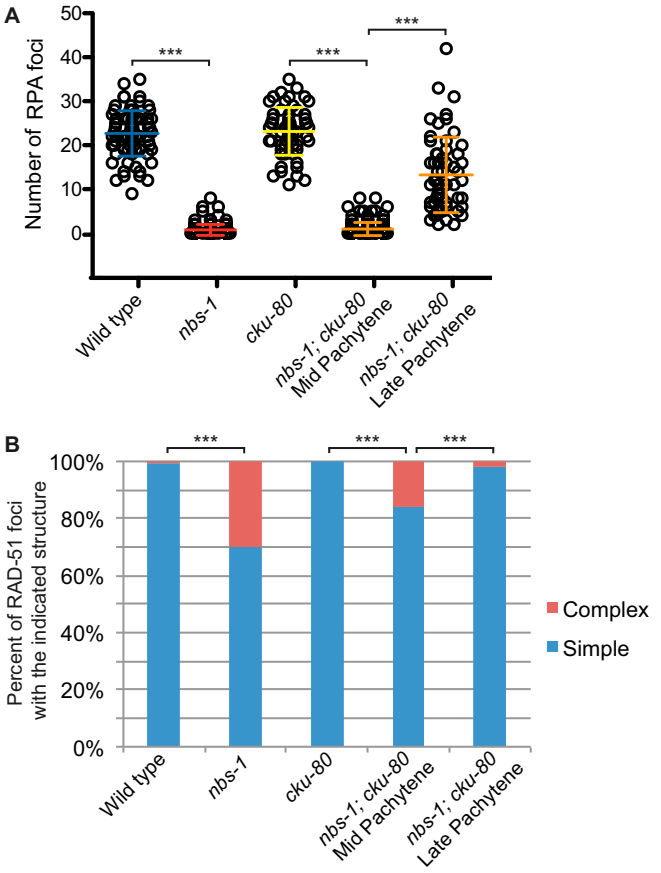

Fig. S4. Quantitation of foci in spread nuclei. (*A*) Scatterplots depicting quantiation of numbers of YFP::RPA-1 (RPA) foci in pachytene nuclei from spread gonads of the indicated genotypes (*Materials and Methods*), with each point representing the number of foci detected in an individual nucleus. Horizontal lines and error bars indicate mean ± SD. Numbers of nuclei scored: WT (80 nuclei from four gonads), *nbs-1* (164 nuclei from three gonads), *cku-80* (60 nuclei from three gonads), *nbs-1; cku-80* mid-pachytene (179 nuclei from three gonads), and *nbs-1; cku-80* late pachytene (65 nuclei from three gonads). No significant differences were detected between WT and *cku-80* or between *nbs-1* and *nbs-1; cku-80* mid-pachytene. ***$P < 0.0001$ (two-tailed Mann–Whitney test). (*B*) Stacked bar graphs indicating the proportions of RAD-51 foci in SIM images of spread nuclei that were scored as simple or complex according to criteria presented in *Materials and Methods*. Numbers of foci scored: WT (200 foci in 37 nuclei), *nbs-1* (46 foci in 90 nuclei), *cku-80* (126 foci in 54 nuclei), *nbs-1; cku-80* mid-pachytene (114 foci in 104 nuclei), and *nbs-1; cku-80* late pachytene (231 foci in 64 nuclei). ***$P < 0.0001$ by Fisher exact test.

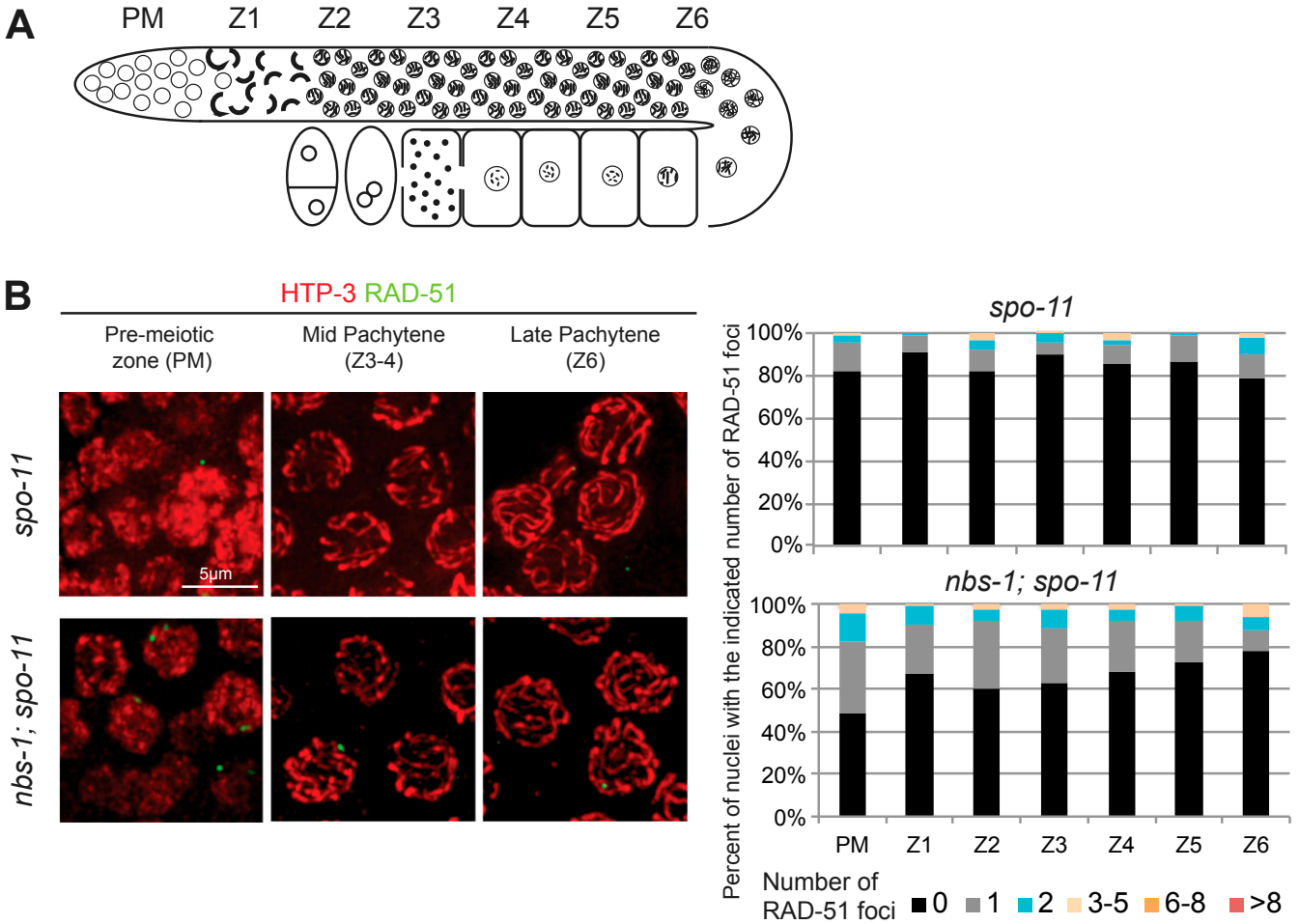

Fig. S5. RAD-51 foci quantitation in *spo-11* and *nbs-1; spo-11* mutants. (*A*) Schematic representation of the spatio-temporal organization of *C. elegans* gonad and the seven consecutives zones from the premeiotic zone (PM) through the end of pachytene (Z6) used to assess RAD-51 foci numbers in whole-mount images in the different mutants throughout this study (more details are in *Materials and Methods*). (*B*, *Left*) Immunolocalization of HTP-3 and RAD-51 in nuclei from whole-mount gonads. (*B*, *Right*) Quantification of RAD-51 foci in the seven consecutive gonad zones defined in *A* in both *spo-11* and *nbs-1; spo-11* mutants.

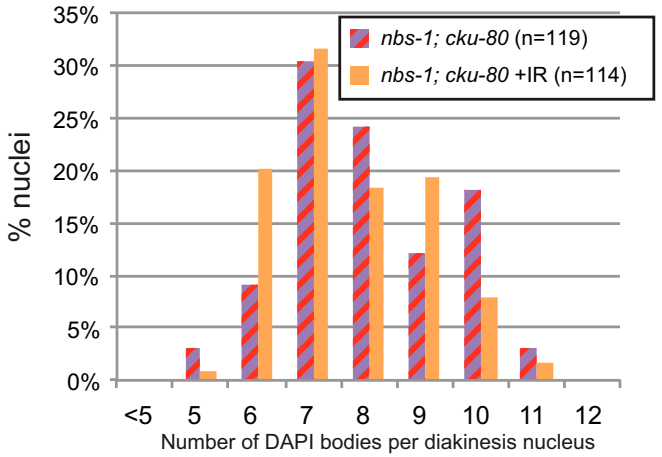

Fig. S6. Quantification of DAPI bodies in diakinesis nuclei in the *nbs-1; cku-80* double mutant exposed to 5,000-rad γ-irradiation (mean 7.7 ± 1.3, $n = 114$) and in the unirradiated control (7.9 ± 1.4, $n = 119$, Mann–Whitney $P = 0.21$). Partial restoration of CO formation in *nbs-1; cku-80* is not improved by excess DSB formation.

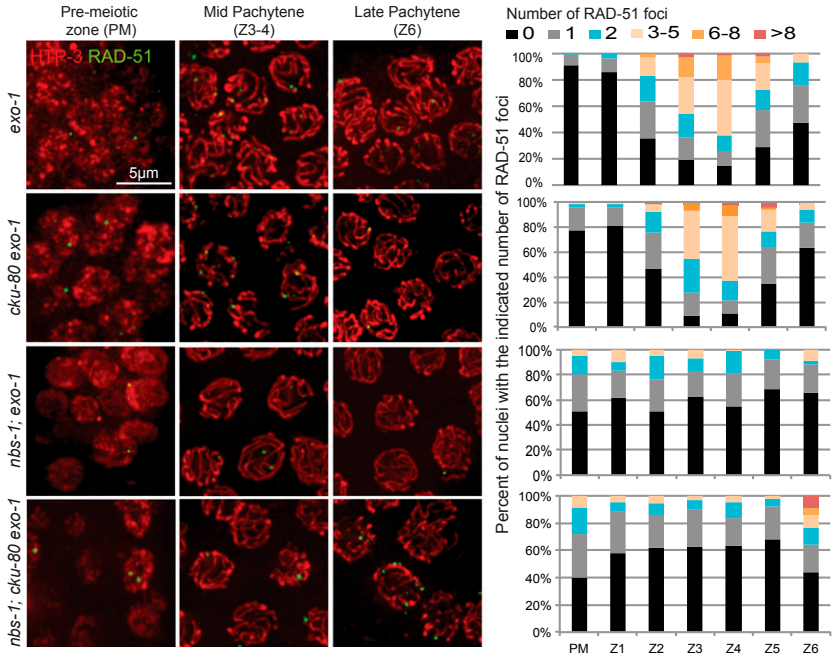

Fig. S7. Immunolocalization of HTP-3 and RAD-51 in whole-mount preparations for the genotypes scored in Fig. 6C.

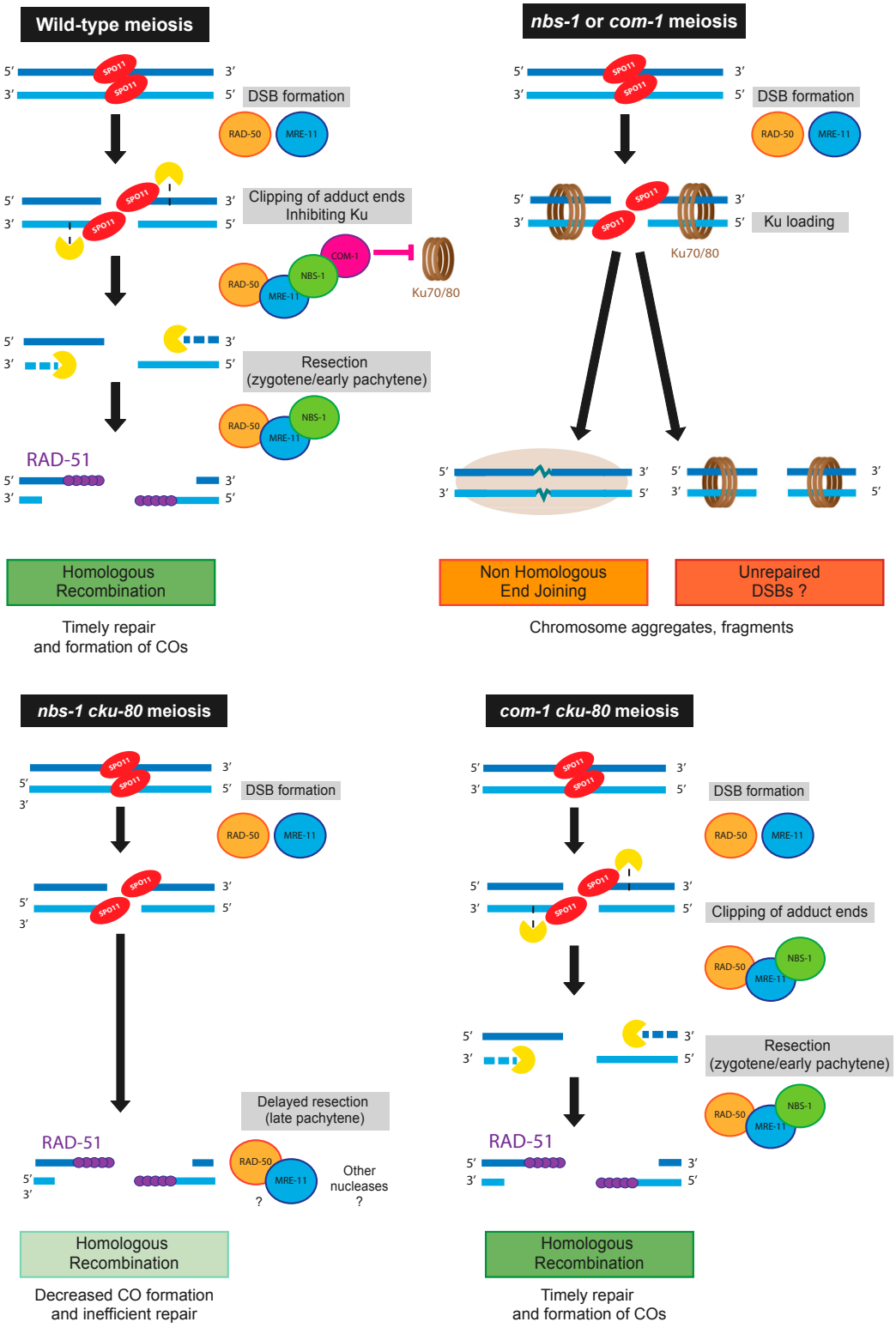

Fig. S8. NBS-1 is essential for COM-1 recruitment to inhibit NHEJ and for MRN function to promote timely resection of DSBs at meiosis. The working model is derived from the findings of this study and others as discussed in the text. The process by which covalently bound SPO-11 might be removed from DSB ends in the *nbs-1* or *com-1* mutant to allow for end ligation is unknown. As Mre11 has been implicated in removing protein–DNA adducts during DNA replication (1), it is possible that MRE-11 nuclease activity could be involved in SPO-11 removal during meiosis even in absence of NBS-1 or COM-1. Alternatively, other enzymes, such as tyrosyl DNA phosphodiesterases, have also been implicated in removing protein–DNA adducts in somatic cells (2) and could also play a role in this case.

1. Lee KC, et al. (2012) MRE11 facilitates the removal of human topoisomerase II complexes from genomic DNA. *Biol Open* 1:863–873.
2. Zeng Z, Cortés-Ledesma F, El Khamisy SF, Caldecott KW (2011) TDP2/TTRAP is the major 5′-tyrosyl DNA phosphodiesterase activity in vertebrate cells and is critical for cellular resistance to topoisomerase II-induced DNA damage. *J Biol Chem* 286:403–409.

Table S1. Quantitation of progeny viability and male frequency

Genotype	Average no. of eggs laid ± SE	No. of broods, *n*	Viable adults, %	Total no. of eggs laid	Males, %
WT	287 ± 5	10	100	2,878	0.05
nbs-1	157 ± 8	10	0	1,575	NA
spo-11	69.4 ± 9	9	9	516	27
nbs-1; spo-11	53.8 ± 9	8	15	366	40
cku-80	204 ± 15	7	100	1,427	0.1
exo-1	225 ± 17	10	100	2,251	0.7
cku-80 exo-1	206 ± 19	10	100	2,065	0.004
nbs-1; cku-80	158 ± 22	19	3.1	3,007	14
nbs-1; exo-1	4 ± 6	19	0	78	NA
nbs-1; cku-80 exo-1	45.5 ± 7	10	0	455	NA

NA, not applicable.